Quality Assessment of TanDEM-X DEM 12m Using GNSS-RTK and Airborne IFSAR DEM: A Case Study of Tuba Island, Langkawi

Pa'suya, F. M.,[1] Talib, N., [1]* Narashid, R. H.,[1] Ahmad Fauzi, A. F.,[1] Amri Mohd, F.[1] and Abdullah, M. A.[2]

[1]Environment and Climate Change Group (ECCG), Faculty of Architecture, Planning and Surveying, Universiti Teknologi MARA, Perlis Branch, Arau Campus, 02600 Arau, Perlis, Malaysia
E-mail: noorf492@uitm.edu.my*
[2]Affinivo Consultant Plt, 43300 Seri Kembangan, Selangor, Malaysia
Corresponding Author

DOI: https://doi.org/10.52939/ijg.v18i5.2389

Abstract
Digital elevation models (DEMs) have been recognized as a primary spatial dataset and essential for numerous scientific applications. The advent of TerraSAR-X for digital elevation measurement (TanDEM-X) has opened a new potential to obtain an accurate DEM. Nowadays, the demand/use of TanDEM-X DEM in scientific applications has become increasingly popular as it offers an alternative to the widely used DEMs: ASTER and SRTM DEM. Although many researches have been conducted to assess the performance of the TanDEM-X DEM at different locations in the world, however, only several multi-regional studies have been performed in Malaysian region. Currently, there are two types of DEMs published by DLR i.e., non-open access (12m and 30m resolution) and open access (90m resolution). In this article, the accuracy of TanDEM-X 12m has been comprehensively and systematically evaluated using 1284 GNSS-RTK control points over Tuba Island and airborne IFSAR-DEM as a reference height. Besides, four available global DEMs: TanDEM-X 90m, AW3D30 DEM, SRTM DEM, and ASTER DEM have also been evaluated to identify the accuracy of TanDEM-X DEM 12m. Based on the evaluation using GNSS-RTK points, TanDEM-X 12m exhibits the highest accuracy with an RMSE of ±1.553m. Unexpectedly, AW3D30 DEM shows a better performance compared to TanDEM-X 90m with RMSE of ±1.964m, followed by SRTM DEM with RMSE of ±3.296m Meanwhile, ASTER DEM exhibits the lowest accuracy with RMSE of ±4.100m The comparison of TanDEM-X 12m and the well-known DEM, SRTM DEM with airborne IFSAR-DEM shows the opposite results. Based on the topographic profile at flat and forest area, the SRTM-DEM exhibits better accuracy than TanDEM-X 12m

Keywords: Global DEM, SRTM, AW3D30, ASTER, TanDEM-X DEM, IFSAR-DEM, GNSS-RTK

1. Introduction

Digital elevation models (DEMs) are a crucial source of data for many environmental applications, such as flood inundation modeling (Sampson et al., 2015 and Archer et al.,2018), coastal flooding (Xu et al.,2021), archaeology (Erasmi et al., 2014), glacier changes (Podgórski et al., 2019), etc. In the simulation of flood inundation using hydrodynamic modeling, higher resolution and accurate DEMs are essentially required to obtain precise flood simulation (Marks and Bates, 2000). Basically, DEMs can be produced using various methods, such as, tachometry, leveling, GNSS survey, remote sensing, etc. However, DEMs derived through remote sensing method are often used, particularly to cover large scale areas. Light detection and ranging (LiDAR) are the remote sensing methods used to generate DEMs. This method is capable in providing extremely high vertical information for large scale areas, able to penetrate the ground surface in vegetated and urban areas (Muhadi et al., 2020), and able to acquire data during cloudy condition. Unfortunately, due to the prohibitive cost, the LiDAR DEM is rarely available (Schumann et al., 2014).

Thanks to several organizations that publish global DEMs data for free and diversify their use in various applications, particularly in areas that are difficult to access for direct field surveys. Nowadays, various global DEMs rendered using remote sensing techniques are available at different resolutions and most of the available models are freely accessible with decent accuracy (Khal et al., 2020). The emergence of satellite-derived DEM, such as Shuttle Radar Topographic Mission (SRTM), Advanced Spaceborne Thermal Emission and Reflection Radiometer (ASTER), Advanced Land Observation Satellite (ALOS), TerraSAR-X add-on for Digital Elevation Measurement (TanDEM-X), etc. have offered inexpensive and accessible DEMs to geoscientists. In general, existing global DEMs are acquired through two approaches, namely satellite stereo images and InSAR techniques (Shetty et al., 2021). Since the available global DEMs today is produced from different sources of data and methods, it indirectly influences the accuracy of the DEMs. Therefore, it is crucial to study the vertical accuracy of the DEMs to ensure it meets the accuracy requirements. Literature records show the height accuracy of several open-source global DEMs have been studied frequently by comparing the elevation information extracted from the DEMs with a set of reference data, generally called control points derived from topographic map, GNSS, LiDAR, UAV, etc.

Among the available public domain global DEMs, the DEM generated from space radar terrain mission (SRTM DEM) is currently the most widely used in many applications, such as, flood hazard mapping (e.g., Elkhrachy, 2015, Domeneghetti, 2016 and Kim et al., 2019), hydraulic and hydrologic modeling (e.g., Alsdorf et al., 2010 and Sampson et al., 2015), etc. Currently, there are two different models of SRTM DEM freely available to civilians with differences in terms of resolution and provider. The first DEM global model was released by Land Processes Distributed Active Archive Center (LP DAAC) with 1 arc second resolution, while the second model was released by Consultative Group on International Agricultural Research - Consortium for Spatial Information (CGIAR-CSI) with 3 arc-resolution (~90m). Other commonly used global DEM products are Advanced Spaceborne Thermal Emission and Reflection Radiometer (ASTER) DEM. These global DEMs have a wide range of applicability and are used in various scientific studies, such as rainfall modeling (Ahmed Suliman et al., 2014), watershed analysis (Pareta and Pareta, 2011), changes of glacier lakes (Rai and Mishra, 2017), etc.

The ASTER GDEM data product was created at a spatial resolution of 1 arc second and it is a product of a collaborative effort between National Aeronautics and Space Administration (NASA) and Japan’s Ministry of Economy, Trade, and Industry (METI).

ALOS Global Digital Surface Model (AW3D30) and TerraSAR-X DEM (TanDEM-X) are two new global DEMs freely released to civilian and increasingly favored by researchers. The AW3D30 DEM was released by Japan Aerospace Exploration Agency (JAXA) in May 2016 (Tadano et al., 2016) with 1 arc-sec resolution and this global DEM is expected to provide more accurate elevation measurements compared to other global DEMs. Unfortunately, the vertical accuracy assessment of AW3D30 DEM is very limited compared to the SRTM and ASTER DEM, which are earlier released models. Previous investigations of AW3D30 DEM accuracy have revealed that it provides the highest accuracy among the free DEM products available. For example, a comprehensive assessment by Santillan and Makinano-Santillan (2016) in the Philippines using GPS points found that the AW3D30 DEM accuracy is better than SRTM DEM and ASTER DEM with RMSE of ±5.68m. A similar result has also been reported by Jain et al., (2018), which concluded that AW3D30 DEM exhibited the best accuracy compared to the other four available DEM products. Another result by Li and Zhao (2018) is also consistent with the previously mentioned works after evaluating the accuracy of AW3D30 DEM over five typical landforms validation samples across China. They exhibit that the AW3D30 offers the highest accuracy with an RMSE of ±4.81 m. Developed in a public-private partnership between the German Aerospace Center (DLR) and Airbus Defence and Space, TanDEM-X is the latest global digital elevation product obtained using the same technique as SRTM DEM.

The advent of the TanDEM-X DEM has opened a new era in obtaining global and consistent DEM with unprecedented accuracy. As the ASTER DEM only covers latitudes between 83 South and 83 North (Li et al., 2012), while the AWD30 DEM has numerous gaps in both Antarctica and arctic regions (Tadono et al., 2016), the availability of TanDEM-X DEM can be served as an alternative to SRTM DEM. Currently, there are two versions of TanDEM-X offered by DLR i.e., open access and non-open access, which differ in terms of resolution and properties. For the non-open access DEMs, two resolutions are offered by DLR, which are 12m and 30m, meanwhile, for the open access DEM product, the resolution offered is 90m.

The absolute vertical accuracy of TanDEM-X DEM 12m is better than 6m, and it has better performance compared to SRTM DEM (Archer et al., 2018). Since the TanDEM-X DEM is the latest DEM product, the discussion of the vertical accuracy is not as comprehensive as the earlier DEM products (e.g., SRTM, ASTER), especially for the edited version, which is not a free and open-access DEM. Literature records found that several studies have evaluated the vertical accuracy of TanDEM-X DEM 12m (e.g., Feng and Muller, 2016, Gabiri et al., 2018, Grohmann, 2018 and Brosens et al., 2022) using various reference elevation, such as, ICESat points (Rizzoli et al., 2017), GNSS points (Baade and Schmullius, 2016, Rexer and Hirt, 2016 and Pa'suya et al., 2018, 2019), height error maps (HEM) (Gonzalez and Rizzoli, 2018) or Kinematic-GPS (KGPS), and GNSS and LIDAR measurements (Wessel et al., 2018). Wessel et al., (2018) has performed a comprehensive comparison to evaluate the accuracy of TanDEM-X DEM 12m using 14 million KGPS points, 23,951 GPS benchmark, and high-resolution LiDAR based DEMs. The comparison with KGPS point, Wessel et al., (2018) has obtained an RMSE value of 1.29m. Meanwhile, the comparison with GPS benchmark points and LiDAR derived-DEM, the study has reported RMSE values of ±1.1m for short vegetation, ±1.4m for developed vegetation, and ±1.8m for forest areas. Another study by Pa'suya et al., (2019) using 7755 GNSS points over the northern region of Peninsular Malaysia has presented the accuracy of this global DEM is approximately ±3.9m. The comparison of TanDEM-X 12m with other global DEMs by Rexer and Hirt (2016) shows that this model is superior to SRTM or ASTER DEM, which consistent with the result of the latest study by Pa'suya et al., (2019). However, the vertical accuracy of TanDEM-X 12m at flat terrain is similar to the AWD30 (Grohmann, 2018). In recent years, TanDEM-X 90m has become increasingly popular and many authors have started evaluating the model after its release by DLR (e.g., Halim et al., 2018, Ravanelli et al., 2020, Yadav and Bhardwaj, 2022, and Metilda et al., 2020). A comprehensive comparison between TanDEM-X DEM 90m and SRTM DEM has found that the accuracy of TanDEM-X DEM 90m is better than SRTM DEM (Hawker et al., 2018, and Metilda etl., 2020). The latest study by Liu et al., (2022), which evaluates four open global DEMs, namely AW3D30, ASTER, STRM, and TanDEM-X 90m has also demonstrates that TanDEM-X 90m exhibits the highest stability and accuracy.

Although multiple studies have been carried out to identify the accuracy of TanDEM-X DEM in different parts of the world using various kinds of reference data, unfortunately, literature records show that the accuracy assessment of TanDEM-X DEM model in the Malaysia region is scarce. To the the best of author's knowledge, only three studies (Pa'suya et al., 2018, 2019 and Halim et al., 2019) have been conducted focusing on the accuracy assessment of this model using GNSS point as a reference point. Therefore, the aim of this study is to conduct a comprehensive vertical accuracy assessment of the TanDEM-X DEM 12m and 90m using reference height GNSS-RTK point and IFSAR derived DEM. In order to illustrate the significant performance of the TanDEM-X DEM 12m, the DEMs are compared with three available global DEMs i.e. SRTM, ASTER, and AWD30 DEM.

2. Material and Methods

2.1 Description of the Study Area

The area selected for the study is Tuba Island, which located approximately 5km southwest of Langkawi Island, Kedah Malaysia. This island is located among the archipelago of 99 islands. Lies between 6°12′45″ N to 6°16′9″ N latitude and 99°49′15″ E to 99° 51′54″ E longitude (Figure 1) with an area of 1,763 hectares (or 20 square kilometers) makes this human-inhabited island as the third largest island after Langkawi Island and Dayang Bunting Island (Ghazali et al., 2016). Since 2019, Universiti Teknologi MARA, Malaysia has participated in research collaboration with several researchers from other universities to conduct various researches on this island, and one of the ongoing research projects is to study the impact of sea level rise on the coastal inundation over this island. However, the lack of DEM information, which is crucial information in such research has encouraged this study to identify the potential of TanDEM-X DEM product to provide DEM information over this island.

2.2 Global DEMs used in the Study

2.2.1 ALOS World 3D - 30m (AW3D30)

ALOS Global Digital Surface Model, also known as ALOS World 3D - 30m (AW3D30) offers an alternative DEM to the available global DEM. This global DEM model generated between latitudes 80° N and 80° S using the images of Panchromatic Remote-sensing Instrument for Stereo Mapping (PRISM) on board the ALOS (Takaku and Tadono, 2009). By resampling the 5m ALOS DEMs, Japan Aerospace eXploration Agency (JAXA) has generated 1°×1° tiles of 1 arcsec (~30 m) and freely available to the public in 2016 (Tadono et al., 2016).

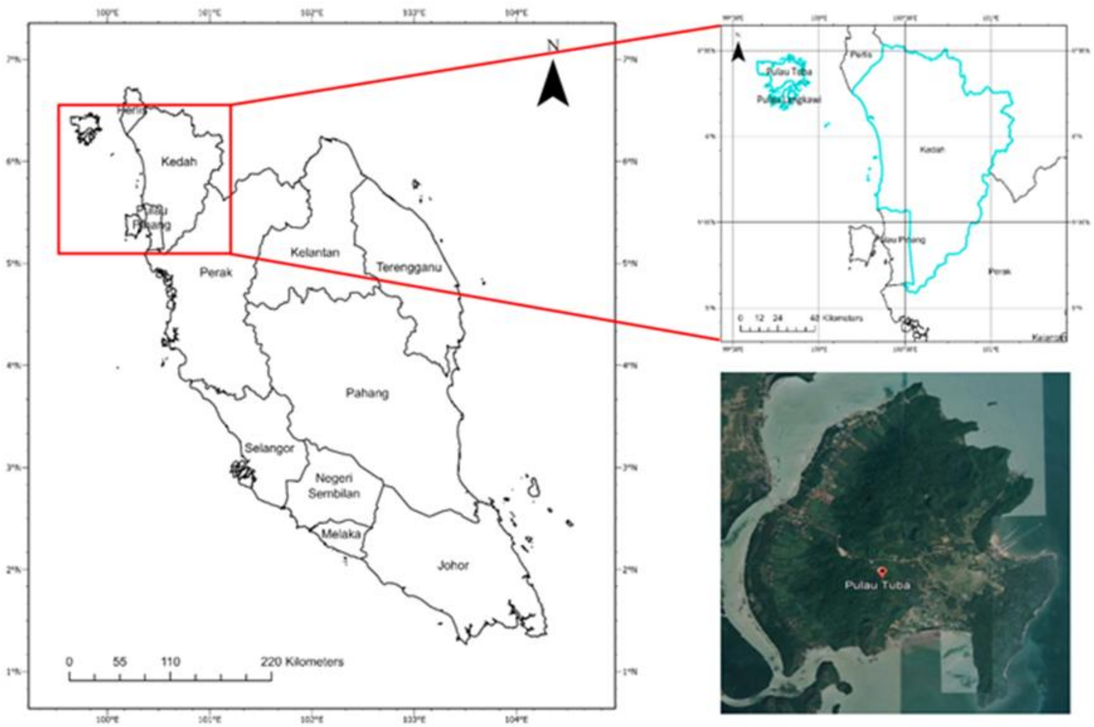

Figure 1: Location of Tuba Island (study area)

In several years, JAXA has upgraded the global DEMs and released a few versions, such as version 2.1 in 2018, version 2.2 in 2019, and version 3.1 in 2021. Recently, JAXA upgraded this DEM to version 3.2 in 2021 with corrected sea mask (https://www.eorc.jaxa.jp/ALOS/en/aw3d30/index.htm, accessed 15 September 2021). This global DEM is referenced to the WGS84 horizontal datum and EGM96 vertical datum. In this study, the AW3D30 DEM of Tuba Island (Figure 2) in GeoTIFF format are downloaded from http://www.eorc.jaxa.jp-/ALOS/en/aw3d30/. There are two resolutions of tiles can be downloaded from the website, which are 1 × 1 degree unit and 5 × 5 degree unit in latitude and longitude. Besides, there are two types of data can be selected by users either AVE (average) or MED (median), however, for this study, AVE tiles with 1 × 1 degree unit are opted.

2.2.2 SRTM DEM

SRTM DEMs were developed using Interferometric Synthetic-Aperture Radar (InSAR) mission aboard the National Aeronautics and Space Administration (NASA) space shuttle in February 2000 (Courty et al., 2019). This global DEM was produced with two spatial resolutions: 3-arc second (~90m) and 1 arc-second (~30 meters). Compared to SRTM 90m, which was freely released to the public priorly, SRTM30m only available to the public after it was released by NASA in 2015. This global DEM was developed based on the C-band radar interferometry employed by the SRTM sensor. The elevation obtained from SRTM DEMs represents the elevations between the bare ground and the top of the canopy. This is because the C-band wave cannot penetrate dense vegetations or buildings. In general, there are three versions of SRTM DEMs have been released by NASA. The latest version is version 3, which was released in 2014. This latest version has been incorporated with topographic data to fill the gaps or voids in the previous versions of the SRTM DEMs model. The vertical and horizontal references of SRTM DEMs are EGM96 geoid and WGS84 (World Geodetic System 1984), respectively (Rodriguez et al., 2005). In this study, SRTM DEMs 1-arcsec used are retrieved from U.S. Geological Survey (USGS) EarthExplorer web-platform (https://earthexplorer.usgs.gov/).

ASTER DEM product was produced in collaboration with the Japanese Ministry of Economy, Trade, and Industry (METI) using data from the ASTER image instrument aboard the Terra satellite. Available with 30m resolution, this DEM product covers the earth surface between 83° North and 83° South and freely released to the public in June 2009.

Although the coverage area of ASTER DEM is wider compared to SRTM DEM, SRTM DEM is still preferred in hydrodynamic modeling as it offers better feature resolution and higher vertical accuracy (Hirt et al., 2010 and Rexer and Hirt, 2014).

2.2.3 ASTER DEM

National Aeronautics and Space Administration (NASA) and METI have joint collaboration and released the second version of ASTER DEM in mid-October 2011, and the latest version, Version 3 was released in August 2019, with significant improvements from the previous versions. Like STRM DEMs, the vertical and horizontal reference of ASTER DEMs are EGM96 geoid and WGS84, respectively, and the data are available on USGS website (https://earthexplorer.usgs.gov/).

2.2.4 TanDEM-X DEM

TanDEM-X DEM is available in two versions, i.e., freely access and non-freely access. Apart from being different in terms of resolution, it is crucial to highlight that the freely access model (90m resolution) is non-edited version and represents a Digital Surface Model (DSM), which means, this version may contain specific artifacts in the terrain caused by the specific characteristics of SAR (e.g., layover and shadow). It presents surfaces including natural and man-made structures. Meanwhile, the TanDEM-X 12m and 30m are the edited versions of the Digital Terrain Model (DTM), in which all the natural and built features have been removed (https://geoservice.dlr.de/web/dataguide/ tdm90/). TanDEM-X 90m is generated from the average values of TanDEM-X 12m (Hawker et al., 2019). In this study, Tandem-X DEM with 12m resolution has been requested from German Aerospace Center (DLR) through research proposal entitled "Towards 1 Centimeter Geoid Model at Southern Region Peninsular Malaysia Using New DEM Model-TanDEM-X". Meanwhile, TanDEM-X 90m is downloaded from DLR website (*https://download. geoservice.dlr.de/TDM90/*). The horizontal and vertical datum of the TanDEM-X (both versions) are referenced to the ellipsoidal height, WGS84 (Wessel et al., 2018). Figure 2 shows the five DEMs over Tuba Island subjected to vertical accuracy assessment and details about each DEMs are presented in Table 1.

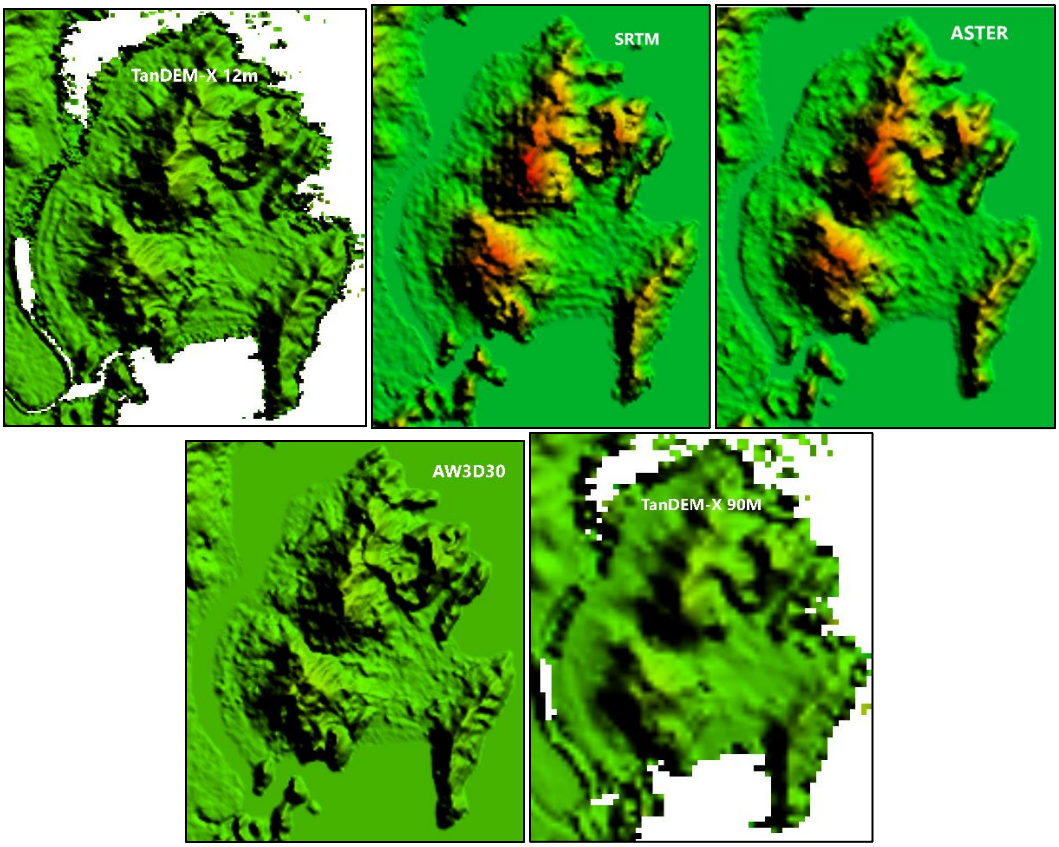

Figure 2: Five DEMs over Tuba Island

Table 1: Overview of global DEMs

Global DEM	Resolution	Vertical Datum	Horizontal Datum	Source
TanDEM-X	12m	WGS84	WGS84	https://tandemx-science.dlr.de/
TanDEM-X	90m	WGS84	WGS84	https://download.geoservice.dlr.de/TDM90/
AWD30	30m	EGM96	GRS80	http://www.eorc.jaxa.jp/ALOS/en/aw3d30/
SRTM	30m	EGM96	WGS84	https://earthexplorer.usgs.gov/
ASTER	30m	EGM96	WGS84	asterweb.jpl.nasa.gov

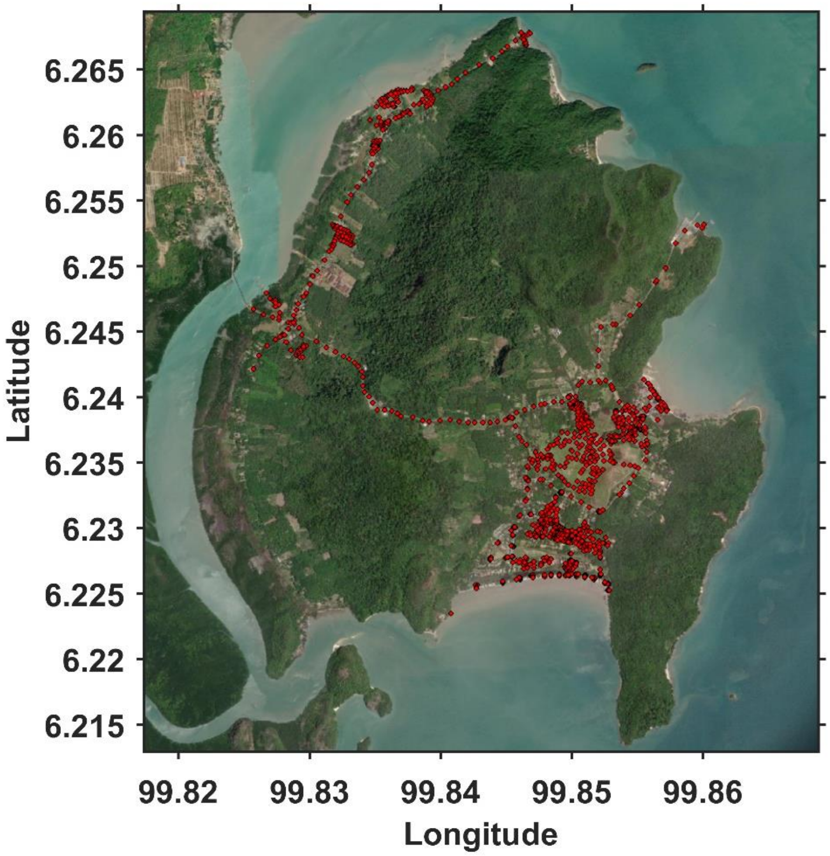

Figure 3: Distributions of the 1284 GNSS RTK point over Tuba Island

2.3 Reference Height for Validation

The accuracy of TanDEM-X 12m and other targeted global DEMs in this study are evaluated using two (2) types of reference height, i.e., height from ground GNSS-RTK survey and height extracted from IFSAR DEM. The sources of both types of height data are described in detail in the following sections.

2.3.1 Ground GNSS survey

GNSS surveys are the widely used method to evaluate global DEMs accuracy (e.g. Erasmi et al., 2014, Patel et al., 2016 and Wessel et al., 2018). In this study, an extensive GNSS campaign has been conducted over Tuba Island using Virtual Reference Station-Real Time Kinematic (VRS-RTK) method. This method is used because it is efficient in obtaining 3D coordinate (φ,ʎ,h) with height accuracy in the range of 1cm to 8cm level accuracy (Sulaiman et al., 2009). A total number of 1284 GNSS RTK points have been acquired during the campaign using Topcon GR5 and the distribution of the points is illustrated in Figure 3. However, the distribution of GNSS points is not uniform due to the topography of the Tuba Island, which is surrounded by mountains and valleys in the western part of the island.

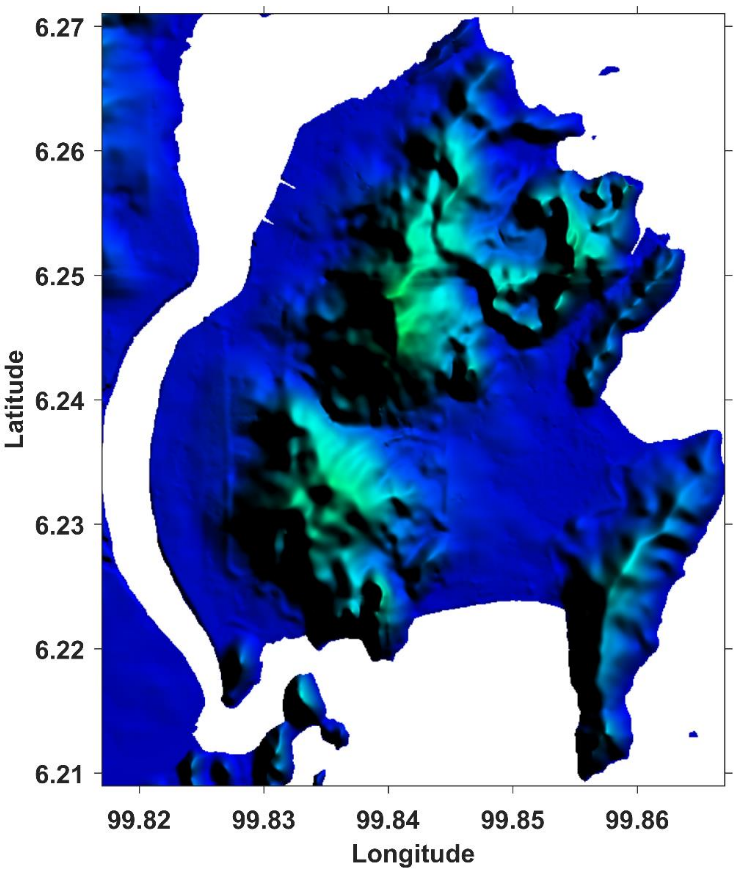

Figure 4: IFSAR DEM over Tuba Island

2.3.2 DEM from Airborne IFSAR

The Tandem-X DEM 12m has also been evaluated using the DEM derived from Interferometric Synthetic Aperture Radar (IFSAR) technologies. These data are provided by the Department of Survey and Mapping Malaysia (DSMM) and details about the DEM can be referred in Zakaria (2018). The IFSAR-generated DEM over Tuba Island is illustrated in Figure 4. To our best knowledge, only several studies have been conducted to examine the accuracy of Airborne IFSAR DEM provided by the DSMM (e.g., Mohd et al., 2014, Hashim and Mohd., 2015 and Mokhtar et al., 2018). According to Mohd et al., (2014), the accuracy of IFSAR DEM, after evaluation using GNSS points, at non-vegetated and vegetated areas are 1.458m and 4.736m, respectively. Meanwhile, another study by Hashim and Mohd (2015) revealed that the accuracy of airborne IFSAR after has been evaluated with GPS points at flat and undulating areas are approximately ±0.497m and ±0.841m, respectively, which is better than SRTM and ASTER DEM. In this study, the DEM information extracted from airborne IFSAR DEMs are used to evaluate the accuracy of DEM from TanDEM-X DEM 12m.

3. Data Processing

3.1 Height Datum Transformation

As mentioned in Table 1, the height value from TanDEM-X DEM (90m and 12m) are corresponding to the ellipsoidal heights, which is referenced to the ellipsoid WGS84-G1150 (Gruber et al., 2012). However, SRTM, ASTER, and AWD30 DEM elevations are corresponding to the orthometric heights, which are referenced to the Geoid EGM96. Therefore, the elevation height, *H*, extracted from the three DEMs product must be transformed to the ellipsoidal height by adding EGM96 geoid undulation, N_{EGM96}, to the orthometric height, *H*, as follows:

$$h_{ellipsoidal} = H + N_{EGM96}$$

Equation 1

The geoid undulation, *N*, value at each grid point is extracted from the EGM96 geoid model using the F477.F program provided by NGA (http://earth-info:nga:mil/GandG/wgs84/gravitymod/egm96/egm96:html).

ISSN: 1686-6576 (Printed) | ISSN 2673-0014 (Online) | © Geoinformatics International

3.3 DEM Accuracy Assessment

DEMs comparison has been conducted based on two assessments: (1) the TanDEM-X DEM (90m and 12m) and other targeted DEM products are compared with reference height, h_{ref}, measured by GNSS, extracted from UAV DEM and airborne IFSAR DEM to estimate the height error, $\Delta h_i = h_i - h_{ref}$; (2) the analysis is focused on the elevation differences between TanDEM-X 12m and each DEM. Here, the DEM accuracy is accessed using mean error (ME), mean absolute error (MAE), root mean square error (RMSE), and standard deviation (STD), as follows (Hawker et al., 2019):

Mean Absolute Error (MAE)

$$MAE = \frac{1}{n}\sum_{i=1}^{n} | h_i - h_{ref}| = \frac{1}{n}\sum_{i=1}^{n} |\Delta h_i |$$

Equation 2

Mean Error (ME)

$$ME = \frac{1}{n}\sum_{i=1}^{n} h_i - h_{ref} = \frac{1}{n}\sum_{i=1}^{n} \Delta h_i$$

Equation 3

Root Mean Square Error (RMSE)

$$RMSE = \sqrt{\frac{1}{n}\sum_{i=1}^{n} \Delta h_i^2}$$

Equation 4

Standard Deviation (STD)

$$STD = \sqrt{\frac{1}{n-1}\sum_{i=1}^{n} (\Delta h_i - ME)^2}$$

Equation 5

where n is the number of points. It is assumed that the vertical errors are normally distributed and at confident levels of 90% (LE90), 95% (LE95), and 99% (LE99), it is calculated as:

$$LE90 = STD\ X\ 1.6449$$
$$LE95 = STD\ X\ 1.9600$$
$$LE99 = STD\ X\ 3.0000$$

Equation 6

4. Result and Discussion

4.1 Comparison between Global DEMs

In this study, the performance of TanDEM-X DEM 12m is assessed through (4) methods: (1) comparison with other global DEM (TanDEM-X 90m, SRTM, ASTER, and AW3D30); (2) comparison with height from GNSS points; (3) comparison with drone-DEM; and (4) comparison with IFSAR DEM. In the first phase, prior to the comparison process, TanDEM-X 12m and 90m are resampled to 30m resolution. The differences between TanDEM-X 12m and global DEMs are illustrated in Figure 5 and the statistical analysis of the differences are listed in Table 2. As expected, the significant differences between TanDEM-X DEM 12m and other global DEMs are over forest areas, but moderate in flat regions, as exhibited in Figure 4. TanDEM-X 90m model shows smaller deviations from TanDEM-X 12m compared to other DEM with an RMSE of ±6.442m and linear error at three confident levels ranging from 10.591m to 19.315m. Surprisingly, based on the statistical analysis, the AW3D30 DEM shows better accuracy than SRTM DEM with RMSE of ±6.670m and linear error at the three confidence levels ranging from 10.971m to 20.009m. Followed by SRTM DEM with an RMSE of ±9.415m and LE ranging from 15.486m to 28.243m. In case of the comparison with ASTER DEM, which shows larger deviation than TanDEM-X 12m, the LE ranges from 18.168m to 33.135m with RMSE of 11.083m.

Table 2: Statistical analysis of the difference between TanDEM-X DEM 12m minus TanDEM-X 90m, AWD30, SRTM, and ASTER DEM [units: meters]

Model	ME	MAE	RMSE	STD	LE90	LE95	LE99
AW3D30	-0.008	4.053	6.670	6.670	10.971	12.672	20.009
SRTM	-0.138	5.962	9.415	9.414	15.486	17.887	28.243
ASTER	0.916	7.626	11.083	11.045	18.168	20.985	33.135
TanDEM-X 90	0.204	4.280	6.442	6.438	10.591	12.233	19.315

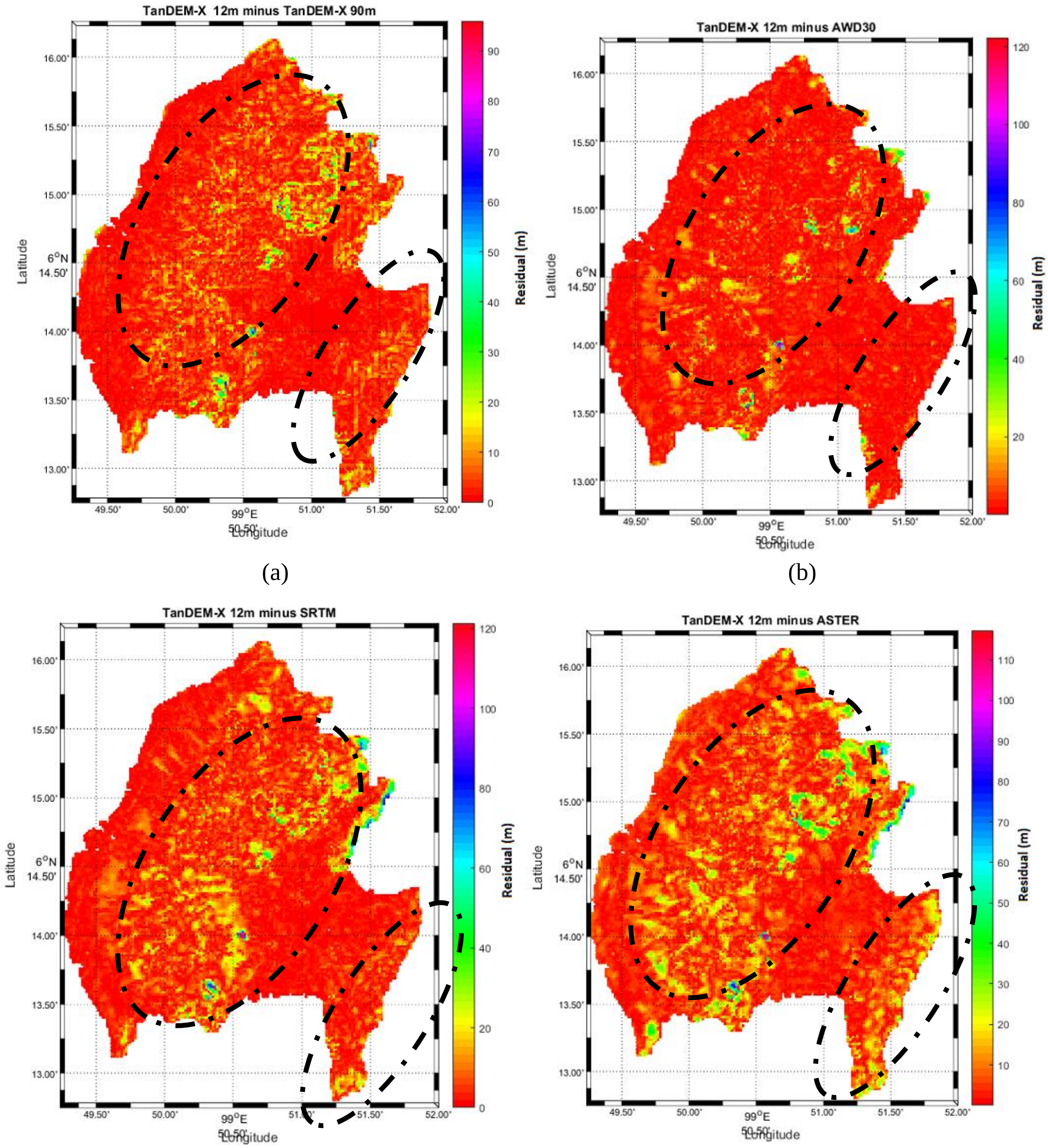

Figure 5: DEM height different between TanDEM-X DEM 12m with (a) TanDEM-X 90m , (b) AWD30 , (c) SRTM, and (d) ASTER. The circles show the forest region over study area

The coefficient of correlation values of height between TanDEM-X DEM 12m and Tandem-X DEM 90m, AWD30m, SRTM DEM, and ASTER DEM are 0.9884, 0.9875,0.9743, and 0.9647, respectively (Figure 6). It can be concluded that all DEMs are highly correlated with TanDEM-X 12m with TanDEM-X DEM 90m having the highest level of agreement. It is expected since this DEM is retrieved from similar platform with the TanDEM-X DEM 12m.

4.2 Comparison with GNSS-RTK

As described in Section 2.3.1, a data set of 1284 RTK-GPS points is used to examine the performance of TanDEM-X DEM and other global DEMs (ASTER , SRTM, and AW3D30 DEM) by comparing their heights with the RTK-GPS derived ellipsoidal height. The outliers among 1284 RTK-GPS points are identified using the 3sigma rule (3σ) and removed from the dataset.

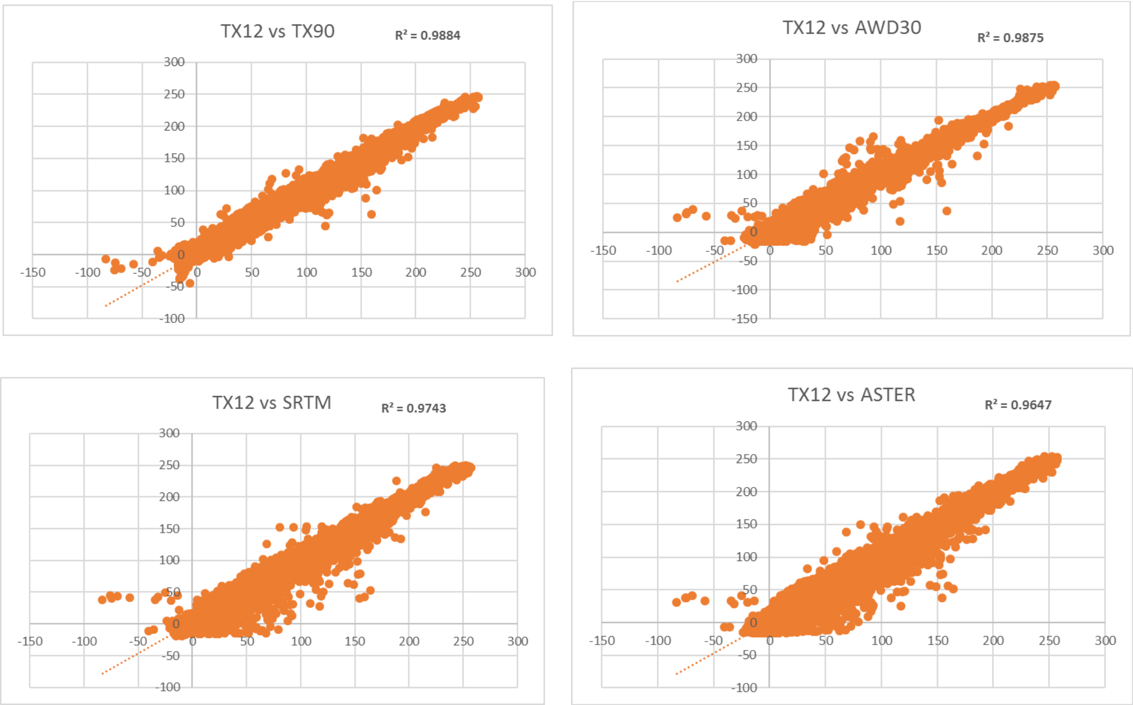

Figure 6: Correlation values between height extracted from TanDEM-X 12m and other global DEM

Table 3 Descriptive statistics evaluation using GNSS- RTK for TanDEM-X 12m, TanDEM-X 90m, SRTM, ASTER, and AW3D30

Model	Min(m)	Max(m)	ME(m)	MAE(m)	RMSE(m)
TanDEM-X 12m	0.002	4.750	0.336	1.190	1.553
TanDEM-X 90m	0.001	7.365	1.297	1.669	2.229
SRTM	0.000	9.816	2.355	2.604	3.296
ASTER	0.016	11.747	3.342	3.492	4.100
AW3D30	0.001	5.55	-1.405	1.694	1.964

The comparison is classified as a flat area assessment since most of RTK GPS points are located in flat regions, as shown in Figure 3. The distribution of height differences between RTK-GPS and DEMs are shown in Figure 7. Meanwhile, the statistical analysis is summarized in Table 3.

As illustrated in Table 3, it can be inferred that TanDEM-X DEM 12m presents the highest accuracy with the lowest RMSE and mean error (ME) of ±1.553m and 0.336m, respectively, followed by AWD30, TanDEM-X DEM 90m, SRTM DEM, and ASETR DEM. These findings are comparable to the results of Wessel et al., (2018), which used a similar model and comparison method. However, it is unexpected that AWD30 DEM has better accuracy with RMSE and ME of ±1.964m and -1.405m, respectively, compared to TanDEM-X DEM 90m (RMSE and ME of ±2.229m and 1.297m, respectively) and SRTM DEM (RMSE and ME of ±3.296m and 2.355m, respectively).

4.3 Comparison with IFSAR-DEM

Undeniably, the GNSS-RTK-derived heights are reliable reference data (Gonzalez-Moradas and Viveen, 2020), however, the distribution of the GNSS points is limited. It also requires high costs to cover large-scale areas and rugged remote regions. DEM derived from raw radar data collected by airborne IFSAR systems is the alternative sources to overcome the limitation of GNSS-RTK surveys. Thus, an extensive validation to verify the accuracy of TanDEM-X 12m is conducted by comparing the data with IFSAR-DEM, provided by the Department of Survey and Mapping Malaysia (DSMM). The orthometric height from IFSAR-DEM is referenced to the local vertical datum. It is considered as reference values in the analysis of differences between DEM. To evaluate the performance of the TanDEM-X 12m, the well-known global DEM, SRTM has also been evaluated using IFSAR-DEM.

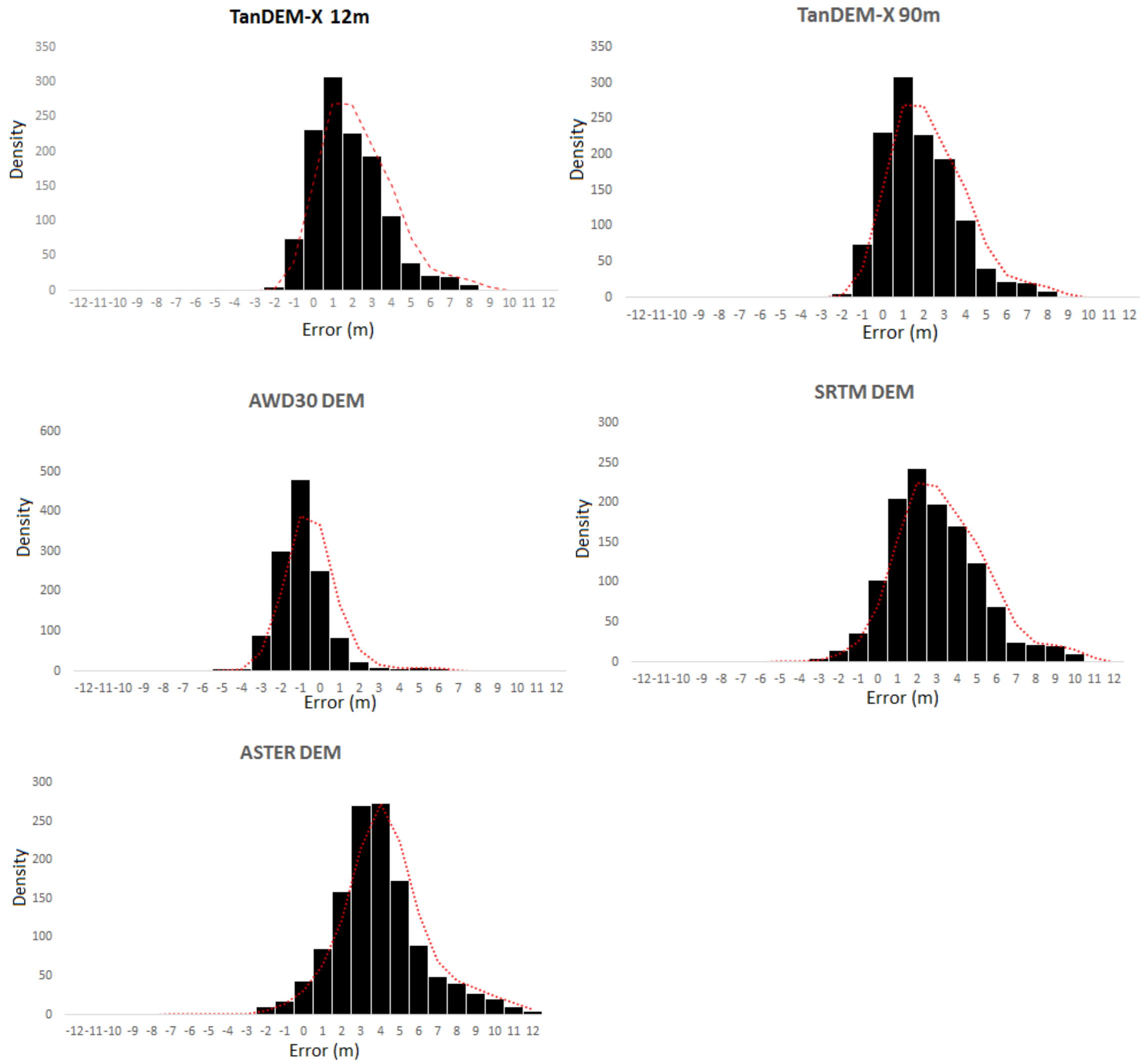

Figure 7: Distribution of 383 First order terrestrial gravity surveys over Peninsular Malaysia for GGM evaluation

The assessment results are discussed in this section. As the IFSAR-DEM and TanDEM-X 12m are referred to different vertical reference system, a conversion has been applied to convert the orthometric height of IFSAR DEM to the ellipsoidal datum to provide a consistent comparison. The conversion was performed by extracting geoidal height from the Malaysian precise geoid model (MyGEOID) and add it to the IFSAR-DEM to derive ellipsoidal height, h_{IFSAR}, as follows:

$$h_{IFSAR} = H_{IFSAR} + N_{MyGEOID}$$

Equation 7

The comparisons are conducted based on topographical profiles in two different areas; forest (Profile 1) and flat area (Profile 2), as shown in Figure 8. The topographic profile from the three sources of DEMs are plotted for the elevation comparison (Figure 9). Surprisingly, the comparison with IFSAR DEM at flat area shows that SRTM DEM outperforms the TanDEM-X 12m. Statistical analysis as listed in Table 4 shows the SRTM DEM generated higher accuracy with ME, STD, and RMSE of -0.256m, ±1.872m, and ±1.888m, respectively. Meanwhile, for the TanDEM-X 12m, comparison with IFSAR DEM shows the ME, STD, and RMSE are 0.723m, ±1.938m, and ±2.068m, respectively.

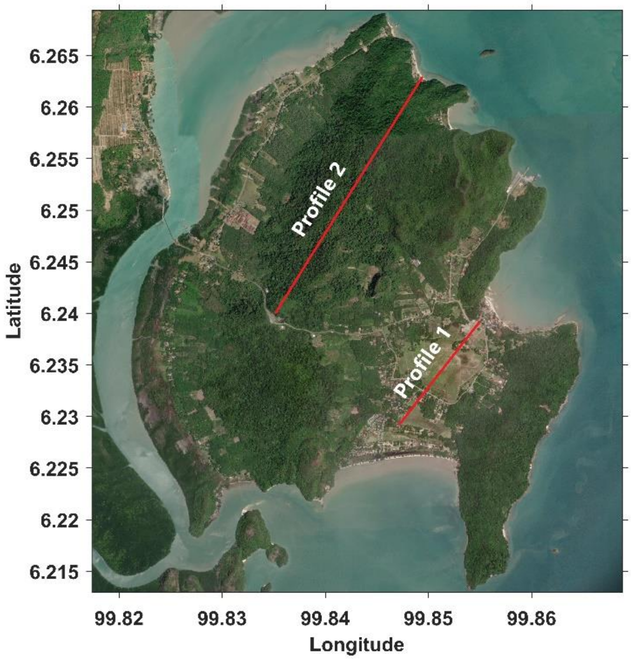

Figure 8: Topographic profile location for the flat area (Profile 1) and forest area (Profile 2)

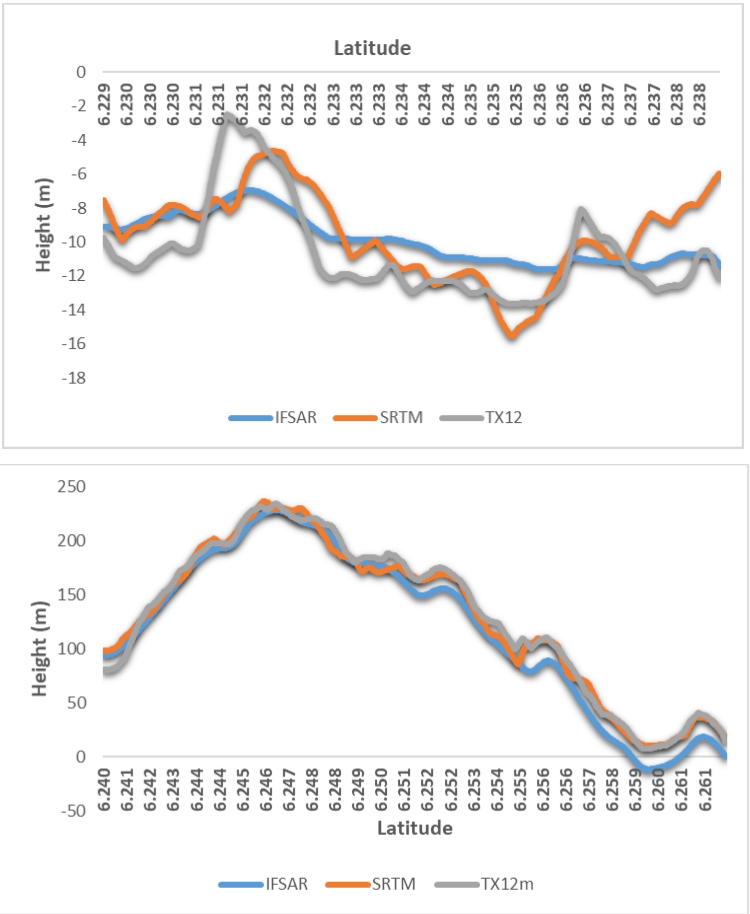

Figure 9: Topographic profiles of three different sources of DEM at flat area (upper) and forest area (below)

Table 4: Statistical analysis of error metric for SRTM DEM and TanDEM-X 12m

Profile	DEM Model	Mean Error (m)	STD (m)	RMSE (m)
Profile 1 (Flat)	SRTM	-0.256	±1.872	±1.888
	TANDEM-X 12M	0.723	±1.938	±2.068
Profile 2 (Forest)	SRTM	10.807	±7.072	±12.913
	TANDEM-X 12M	12.740	±6.607	±14.350

In the forest area, the deviation from the IFSAR DEM for both DEM (TanDEM-X 12m and SRTM DEM) is insignificant (above and below IFSAR DEM) compared to the topographic profile in flat area, as illustrated in Figure 9. Comparison with the IFSAR DEMshows the SRTM DEM elevation along the forest area is closer to the IFSAR DEM with ME, STD, and RMSE of 10.807m, ±7.072m, and ±12.913m, respectively, outperforming TanDEM-X 12m. with RMSE, ME, and STD of ±14.350m, 12.740m, and ±6.607m, respectively. In general, the result from the statistical analysis is unexpected because the comparison with GNSS-RTK results indicates that TanDEM-X 12m is clearly outperform SRTM. However, this comparison is possibly unreliable as the accuracy of IFSAR DEM in this area may be considered ‘unknown’. Additionally, IFSAR DEM and SRTM DEM are generated using identical mapping system i.e., Interferometric Synthetic Aperture Radar.

5. Conclusion

This study presents a comprehensive accuracy assessment of TanDEM-X DEM 12m at Tuba Island using RTK-GPS and IFSAR DEM. In the first assessment, the TanDEM-X 12m is compared with four available global DEMs, i.e., TanDEM-X 90m, ASTER DEM, SRTM DEM, and AW3D30. The results show that the comparison with TanDEM-X 90m is more accurate than other DEMs in terms of vertical error with an RMSE of ±6.442m. It has been expected since both DEMs are generated from an identical data acquisition method. However, comparison with AW3D30 DEM provides almost similar accuracies with TanDEM-X DEM 90m, with an RMSE of ±6.670m, followed by SRTM DEM and ASTER DEM with RMSE of ±9.415m and ±11.083m, respectively. Further investigation, reveals that TanDEM-X 12m has the highest correlation with TanDEM-X 90m, followed by AW3D30, SRTM DEM, and ASTER DEM. The next comparison is performed using 1284 GNSS-RTK points. The results show that TanDEM-X DEM 12m outperforms other DEMs with an RMSE of ±1.553m. Surprisingly, the results also indicate that AW3D30 DEM provides reasonably better accuracy than TanDEM-X 90m, SRTM, and ASTER DEM with RMSE of ±1.964m. However, TanDEM-X 90m outperforms SRTM DEM and ASTER DEM with RMSE of ±2.229m. In the last assessment, TanDEM-X 12m and SRTM DEM are compared with airborne IFSAR-DEM based on the topographic profile at two different land covers i.e., flat and forest area. All the three DEMs (IFSAR, TanDEM, and SRTM) are obtained using similar data acquisition method, which is SAR technology. Comparison at flat and forest area reveal the topographic profile generated from SRTM DEM outperform TanDEM-X 12m. It is an unexpected result and further investigations are required. One of the arguments is the accuracy of IFSAR-DEM itself should be verified, particularly after conversion from the orthometric height to ellipsoidal height. From this result, it can be concluded that the vertical accuracy does not merely depends on the resolution of DEM, as the results indicate 90m resolution of TanDEM-X perform better than the 30m resolution of SRTM and ASTER. Data acquisition method could be the major influence of increasing DEMs accuracy. AW3D30 DEM sets a new milestone in the current freely available global DEMs and can be a better alternative DEM to TanDEM-X 12m, which is not a free and open-access DEM.

Acknowledgment

Special thanks to Universiti Teknologi MARA (UiTM) for the financial funding through Lestari SDG@Triangle 2.0 Research Grant- Reference code: 600-RMC/LESTARI SDG-T 5/3 (103/2019). We are also grateful to the Department of Survey and Mapping Malaysia (DSMM) for providing the IFSAR DEM through NAHRIM over Tuba Island. The authors would also like to thank the German Aerospace Center (DLR) for providing the TanDEM-X DEM with 12m resolution under the project ―Towards 1 Centimetre Geoid Model at Southern Region Peninsular Malaysia using the New DEM Model- TanDEM-X‖ (Proposal ID: DEM_OTHER1156).

Refereneces

Archer, L., Neal, J. C., Bates, P. D. and House, J. I., 2018, Comparing TanDEM-X Data with Frequently Used DEMs for Flood Inundation Modeling. *Water Resources Research*, Vol. 54(12), 10,205-10,222. https://doi.org/10.1029/-2018WR023688.

Alsdorf, D. E., Han, S. C., Bates, P. D. and Melack, J., 2010, Seasonal Water Storage on the Amazon Floodplain Measured from Satellites. *Remote Sensing of Environment*, Vol. 114(11), 2448 - 2456. https://doi.org/10.1016/j.rse.2010.05.020.

Ahmed Suliman, A. H., Gumindoga, W., Katimon, A. and Darus, I. Z. M., 2014, Semi-distributed Rainfall-Runoff Modeling Utilizing ASTER DEM in Pinang Catchment of Malaysia. *Sains Malaysiana*, Vol. 43(9), 1379–1388.

Baade, J. and Schmullius, C., 2016, TanDEM-X IDEM Precision and Accuracy Assessment Based on a Large Assembly of Differential GNSS Measurements in Kruger National Park, South Africa. *ISPRS Journal of Photogrammetry and Remote Sensing*, Vol. 119, 496–508. https://doi.org/10.1016/j.isprsjprs.2016.05.005.

Brosens, L., Campforts, B., Govers, G., Aldana-Jague, E., Razanamahandry, V. F., Razafimbelo, T., Rafolisy, T. and Jacobs, L., 2022, Comparative Analysis of the Copernicus, TanDEM-X, and UAV-SfM Digital Elevation Models to Estimate Lavaka (Gully) Volumes and Mobilization Rates in the Lake Alaotra Region (Madaga.scar). *Earth Surface Dynamics*, Vol. 10(2), 209–227. https://doi.org/10.51-94/esurf-10-209-2022.

Courty, L. G., Soriano-Monzalvo, J. C. and Pedrozo-Acuña, A., 2019, Evaluation of Open-Access Global Digital Elevation Models (AW3D30, SRTM, and ASTER) for Flood Modelling Purposes. *Journal of Flood Risk Management*, Vol. 12(S1). https://doi.org/-10.1111/jfr3.12550.

Domeneghetti, A., 2016, On the use of SRTM and Altimetry Data for Flood Modeling in Data-Sparse Regions. *Water Resources Research*, Vol. 52(4), 2901–2918. https://doi.org/10.1002/-2015WR017967.

Erasmi, S., Rosenbauer, R., Buchbach, R., Busche, T. and Rutishauser, S., 2014, Evaluating the Quality and Accuracy of TanDEM-X Digital Elevation Models at Archaeological Sites in the Cilician Plain, Turkey. *Remote Sensing*, Vol. 6(10), 9475–9493. https://doi.org/10.3390/rs6-109475.

Elkhrachy, I., 2018, Vertical Accuracy Assessment for SRTM and ASTER Digital Elevation Models: A Case Study of Najran City, Saudi Arabia. *Ain Shams Engineering Journal*, Vol. 9(4), 1807–1817. https://doi.org/10.1016/j.asej-.2017.01.007.

Feng, L. and Muller, J. P., 2016, ICESat Validation of TanDEM-X I-DEMS over the UK. *International Archives of the Photogrammetry, Remote Sensing and Spatial Information Sciences - ISPRS Archives*. Vol. 41, 129–136. https://doi.org/10.5194/isprsarchives-XLI-B4-129-2016.

Gabiri, G., Diekkrüger, B., Leemhuis, C., Burghof, S., Näschen, K., Asiimwe, I. and Bamutaze, Y., 2018, Determining Hydrological Regimes in an Agriculturally used Tropical Inland Valley Wetland in Central Uganda Using Soil Moisture, Groundwater, and Digital Elevation Data. *Hydrological Processes*, Vol. 32(3), 349–362. https://doi.org/10.1002/hyp.11417.

Ghazali, N., Ibrahim, N. and Md Yusoff, M. F., 2016, Pembangunan Etos Budaya Etnik Melayu Mengharungi Pemodenan: Kajian Kes Di Pulau Tuba, Langkawi. *Proceedings of The ICECRS*, Vol. 1(1), 1083-1094, https://doi.org/10.21-070/picecrs.v1i1.651.

Gonzalez, C. and Rizzoli, P., 2018, Landcover-Dependent Assessment of the Relative Height Accuracy in TanDEM-X DEM Products. *IEEE Geoscience and Remote Sensing Letters*, Vol. 15(12), 1892–1896. https://doi.org/10.1109/-LGRS.2018.2864774.

González-Moradas, M. del R. and Viveen, W. 2020, Evaluation of ASTER GDEM2, SRTMv3.0, ALOS AW3D30 and TanDEM-X DEMs for the Peruvian Andes against highly accurate GNSS ground control points and geomorphological-hydrological metrics. *Remote Sensing of Environment*, Vol. 237. https://doi.org/10.1016-/j.rse.2019.111509.

Grohmann, C. H., 2018, Evaluation of TanDEM-X DEMs on Selected Brazilian Sites: Comparison with SRTM, ASTER GDEM and ALOS AW3D30. *Remote Sensing of Environment*, Vol. 212, 121-133. https://doi.org/10.1016/j.rse.20-18.04.043.

Gruber, A., Wessel, B., Martone, M. and Roth, A., 2016, The TanDEM-X DEM Mosaicking: Fusion of Multiple Acquisitions Using InSAR Quality Parameters. *IEEE Journal of Selected Topics in Applied Earth Observations and Remote Sensing*, Vol. 9(3), 1047–1057. https://doi.org/10.1109/JSTARS.2015.2421879.

Halim, S. M. A., Green, M. F. P. S., Narashid, R. H. and Din, A. H. M., 2019, Accuracy Assessment of TanDEM-X 90 m Digital Elevation Model in East of Malaysia Using GNSS/Levelling. *Proceeding ICSGRC 2019 - 2019 IEEE 10th Control and System Graduate Research Colloquium*. Institute of Electrical and Electronics Engineers Inc., 88–93, https://doi.org/10.1109/ICSGRC.2019.8837059.

Hashim, S. and Mohd, W. M. N. W., 2015, Evaluation of Vertical Accuracy of Airborne IFSAR and Open Source Digital Elevation Models (DEMs) Based on GPS Observation. *International Journal of Computing, Communication and Instrumentation Engineering*, Vol. 2(2). https://doi.org/10.15242-/ijccie.d0315014.

Hawker, L., Neal, J. and Bates, P., 2019, Accuracy Assessment of the TanDEM-X 90 Digital Elevation Model for Selected Floodplain Sites. *Remote Sensing of Env*ironment, Vol. 232, https://doi.org/10.1016/j.rse.2019.111319.

Hirt, C., Filmer, M. S. and Featherstone, W. E., 2010, Comparison and Validation of the Recent Freely Available ASTER-GDEM ver1, SRTM ver4.1 and GEODATA DEM-9s ver3 Digital Elevation Models over Australia. *Australian Journal of Earth Sciences*, Vol. 57(3), 337–347. https://doi.org/10.1080/08120091003677553.

Jain, A. O., Thaker, T., Chaurasia, A., Patel, P. and Singh, A. K., 2018 Vertical Accuracy Evaluation of SRTM-GL1, GDEM-V2, AW3D30 and CartoDEM-V3.1 of 30-m Resolution with Dual Frequency GNSS for Lower Tapi Basin India. *Geocarto Int.*, Vol. 33, 1237–1256.

Khal, M., Algouti, A., Ahmed, A., Akdim, N., Stankevich, S. and Menenti, M., 2020, Evaluation of Open Digital Elevation Models: Estimation of Topographic Indices Relevant to Erosion Risk in the Wadi M'Goun Watershed, Morocco. *AIMS Journal*, Vol. 6, 231-257. 10.3934/geosci.2020014.

Kim, D. E., Gourbesville, P. and Liong, S. Y., 2019, Overcoming Data Scarcity in Flood Hazard Assessment Using Remote Sensing and Artificial Neural Network. Smart Water, Vol. 4(2), https://doi.org/10.1186/s40713-018-0014-5.

Li, H. and Zhao, J., 2018, Evaluation of the Newly Released Worldwide AW3D30 DEM over Typical Landforms of China Using Two Global DEMs and ICESat/GLAS Data. *IEEE Journal of Selected Topics in Applied Earth Observations and Remote Sensing*, Vol. 11(11), 4430–4440. https://doi.org/10.1109/JSTARS.2018.2874361.

Liu, X., Ran, M., Xia, H. and Deng, M., 2022, Evaluating Vertical Accuracies of Open-Source Digital Elevation Models over Multiple Sites in China Using GPS Control Points. *Remote Sensing*, Vol. 14, https://doi.org/10.3390-/rs14092000.

Li, P., Shi, C., Li, Z., Muller, J. P., Drummond, J., Li, X., Li, T., Li,Y. and Liu, J., 2012, Evaluation of ASTER Gdem Ver2 Using GPS Measurements and SRTM Ver4.1 in China. *ISPRS Annals of the Photogrammetry, Remote Sensing and Spatial Information Sciences*, Vol. 1, 181–186. https://doi.org/10.5194/isprsannals-I-4-181-2012.

Marks, K. and Bates, P., 2000, Integration of High‐Resolution Topographic Data with Floodplain Flow Models. *Hydrological Processes*, Vol. 14(1112), 2109–2122. https://-doi.org/10.1002/1099-1085(20000815/30).

Metilda, E., Khatriker, S., Bhardwaj, A. and Gupta, K., 2020, Accuracy Assessment of Open Accessible Digital Elevation Models in Urban Areas. National Seminar on Recent Advances in Geospatial Technology & Applications. *ISRS.*, 88–93.

Mohd, W. M. N. W., Abdullah, M. A. and Hashim, S., 2014, Evaluation of Vertical Accuracy of Digital Elevation Models Generated from Different Sources : Case Study of Ampang and Hulu Langat. *FIG Congress 2014 Engaging the Challenges – Enhancing the Relevance*. 1–17.

Mokhtar, E. S., Pradhan, B., Ghazali, A. H. and Shafri, H. Z. M., 2019, Assessing Vertical Accuracy and the Impact of Water Surface Elevation from Different DEM Datasets. *Lecture Notes in Civil Engineering*, Vol. 9, 849–862. Springer. https://doi.org/10.1007/978-981-10-8016-6_61.

Muhadi, N. A., Abdullah, A. F., Bejo, S. K., Mahadi, M. R. and Mijic, A., 2020, The use of LiDAR-derived DEM in Flood Applications: A Review. *Remote Sensing*, Vol. 12(14), https://doi.org/10.3390/rs12142308.

Pareta, K. and Pareta, U., 2011, Quantitative Morphometric Analysis of a Watershed of Yamuna Basin, India Using ASTER (DEM) Data and GIS. *International Journal of Geomatics and Geosciences*, Vol. 2(1), 248–269.

Pa'suya, M. F., Din, A. H. M., Amin, Z. M., Rusli, N., Othman, A. H., Aziz, M. A. C. and Samad, M. A. A., 2018, Accuracy Assessment of TanDEM-X DEM and Global Geopotential Models for Geoid Modeling in the Southern Region of Peninsular Malaysia. Proceedings of the Second International Conference on the Future of ASEAN (ICoFA) 2017. *Springer Singapore*, Vol. 2, 91–100. https://doi.org/10-.1007/978-981-10-8471-3_9.

Pa'suya, M. F., Bakar, A. F. A., Din, A. H. M., Aziz, M. A. C., Samad, M. A. A. and Mohamad, M. I., 2019, Accuracy Assessment of the tandem-X DEM in the Northwestern Region of Peninsular Malaysia using GPS-levelling. *ASM Science Journal*, Vol. 12(2), 100–106.

Patel, A., Katiyar, S. K. and Prasad, V., 2016, Performances Evaluation of Different Open Source DEM using Differential Global Positioning System (DGPS*). Egyptian Journal of Remote Sensing and Space Science*, Vol. 19(1), 7–16. https://doi.org/10.1016/j.ejrs.-2015.12.004.

Podgórski, J., Kinnard, C., Pętlicki, M. and Urrutia, R., 2019, Performance Assessment of TanDEM-X DEM for Mountain Glacier Elevation Change Detection. *Remote Sensing*, Vol. 11(2). https://doi.org/10.3390/rs11020187.

Rai, P. K. and Mishra, V. N., 2017, Changes of Glacier Lakes Using Multi-Temporal Remote Sensing Data: A Case Study from India. *Geographica Pannonica*, Vol. 21(3), 132–141. https://doi.org/10.5937/GeoPan1703132K.

Ravanelli, R., Nascetti, A. and Crespi, M., 2020, Large Scale Assessment of Free Global DEMs Through the Google Earth Engine Platform. *International Geoscience and Remote Sensing Symposium (IGARSS)*, 5242–5245 https://doi-.org/10.1109/IGARSS39084 .2020.9324100

Rizzoli, P., Martone, M., Gonzalez, C., Wecklich, C., Borla Tridon, D., Bräutigam, B., Bachmann, M., Schulze, D., Fritz, T., Huber, M., Wessel, B., Krieger, G., Zink, M. and Moreira, A., 2017, Generation and Performance Assessment of the Global TanDEM-X Digital Elevation Model. *ISPRS Journal of Photogrammetry and Remote Sensing*, Vol. 132, 119–139. https://doi.org/-10.1016/j.isprsjprs.2017.08.008.

Rexer, M. and Hirt, C., 2016, Evaluation of Intermediate TanDEM-X Digital Elevation Data Products Over Tasmania Using Other Digital Elevation Models and Accurate Heights from the Australian National Gravity Database. *Australian Journal of Earth Sciences*, Vol. 63(5), 599–609. https://doi.org/10.1080/0812-0099.2016.1238440.

Rodriguez, E., Morris, C. S., Belz, J. E., Chapin, E. C., Martin, J. M., Daffer, W. and Hensley, S., 2005, *An Assessment of the SRTM Topographic Products, Technical Report JPL D-31639, Jet Propulsion Laboratory*, *Pasadena*, *California*. 1-143. Available on http://www2.jpl.nasa.gov/-srtm/SRTM_D31639.pdf.

Sampson, C. C., Smith, A. M., Bates, P. B., Neal, J. C., Alfieri, L. and Freer, J. E., 2015, A High-Resolution Global Flood Hazard Model. *Water Resources Research*, Vol. 51(9), 7358–7381. https://doi.org/10.1002/2015WR016954.

Schumann, G. J. P., Bates, P. D., Neal, J. C. and Andreadis, K. M., 2014, Technology: Fight Floods on a Global Scale. Nature. Vol. 507(7491), https://doi.org/10.1038/507169e.

Shetty, S., Vaishnavi, P. C., Umesh, P. and Shetty, A., 2022, Vertical Accuracy Assessment of Open Source Digital Elevation Models Under Varying Elevation and Land Cover in Western Ghats of India. *Modeling Earth Systems and Environment*, Vol. 8(1), 883–895. https://doi.org/10.1007/s40808-021-01119-2.

Santillan, J. R. and Makinano-Santillan, M., 2016, Vertical Accuracy Assessment of 30-M Resolution ALOS, ASTER, and SRTM global DEMS over Northeastern Mindanao, Philippines. *International Archives of the Photogrammetry, Remote Sensing and Spatial Information Sciences - ISPRS Archives*, 41,–156. International Society for Photogrammetry and Remote Sensing. https://doi.org/10.5194/ispr-sarc-hives-XLI-B4-149-2016.

Sulaiman, S. A. H., Mustafar, M. A., Ali, T. A. T., Abbas, M. A. and Shafri, H. Z. M., 2009, Practical Accuracy of VRS RTK Outside the Malaysian Real Time Kinematic Network (MyRTKnet). *Proceedings of 2009 5th International Colloquium on Signal Processing and its Applications*, *CSPA 2009*, 395–399. https://doi.org/10.1109/CSPA.2009.5069258

Takaku, J. and Tadono, T., 2009, High Resolution DSM Generation from ALOS PRISM - Status Updates on over Three Year Operations. *International Geoscience and Remote Sensing Symposium (IGARSS)*, Vol. 3. https://doi.org/-10.1109/IGARSS.2009.5417878.

Tadono, T., Nagai, H., Ishida, H., Oda, F., Naito, S., Minakawa, K. and Iwamoto, H., 2016, Generation of the 30 M-MESH Global Digital Surface Model by Alos Prism. *International Archives of the Photogrammetry, Remote Sensing and Spatial Information Sciences - ISPRS Archives*, Vol. 41, 157–162, https://doi.org/10.5194/isprsarchives-XLI-B4-157-2016.

Wessel, B., Huber, M., Wohlfart, C., Marschalk, U., Kosmann, D. and Roth, A., 2018, Accuracy Assessment of the Global TanDEM-X Digital Elevation Model with GPS Data. *ISPRS Journal of Photogrammetry and Remote Sensing*, Vol. 139, 171–182. https://doi.org/10.1016/j.isprsjprs.2018.02.017.

Xu, K., Fang, J., Fang, Y., Sun, Q., Wu, C. and Liu, M., 2021, The Importance of Digital Elevation Model Selection in Flood Simulation and a Proposed Method to Reduce DEM Errors: A Case Study in Shanghai. *International Journal of Disaster Risk Science*, Vol. 12(6), 890–902. https://doi.org/10.1007/s13753-021-00377-z.

Yadav, U. and Bhardwaj, A., 2022, Accuracy Assessment of TanDEM-X 90 and CartoDEM Using ICESat-2 Datasets for Plain Regions of Ratlam City and Surroundings. Eng. Proc., Vol. 59, 1-6, https://doi.org/10.3390/ecsa-8-11441.

Zakaria, A., 2018, Application of Ifsar Technology in Topographic Mapping: JUPEM's Experience. *Proceedings of the ICA*, Vol. 1, 1–4. https://doi.org/10.5194/ica-proc-1-125-2018.